Conformational selection of non-hydrolyzable glycomimetics: the conformation of *N*,*N*′-diacetylthiochitobiose bound to wheat germ agglutinin

José Luis Muñoz,[a] Alicia García-Herrero,[a] Juan Luis Asensio,[a] F.-Isabelle Auzennaeau,[b] F. Javier Cañada[a] and Jesús Jiménez-Barbero*[a]

[a] *Instituto de Química Orgánica, CSIC, Juan de la Cierva 3, 28006, Madrid, Spain*
[b] *Dept. of Biochemistry, Pasteur Merieux Connaught, 1755 Steeles Ave West, Toronto, Canada M2R 3T4*

Received (in Cambridge, UK) 25th August 2000, Accepted 26th January 2001
First published as an Advance Article on the web 22nd February 2001

The conformational behaviour of *N*,*N*′-diacetyl-4-thiochitobiose (**1**) has been studied using a combination of NMR spectroscopy (NOE data) and molecular mechanics calculations. Analogies and differences with the natural compound *N*,*N*′-diacetylchitobiose (**2**) have been found. Moreover, the study of its bound conformation to the lectin wheat germ agglutinin has also been studied using TR-NOE experiments. A process of conformational selection is observed and only one of the conformers present in aqueous solution for the free state is bound by the lectin.

Introduction

In recent years, the search for hydrolytically stable sugar mimetics has led to different groups of oligosaccharide analogues with the glycosidic oxygen substituted by heteroatoms.[1] Thus, *C*- and *S*-glycosides may serve as carbohydrate mimics resistant to metabolic processes.[2,3] Nevertheless, for these pseudodisaccharides to be biologically useful, one of the requirements is that their conformational behaviour should be analogous to that of the natural compound, in order to minimize the entropic costs of the recognition process with the receptor.[4] Therefore, it is important to determine how the synthetic derivatives are affected by such modification. In this context, we have recently reported that thiocellobiose is bound by *Streptomyces* sp. β-glucosidase in the conformation usually found for regular *O*-glycosides (*syn*-Φ,Ψ).[5] In contrast, we also have described that the *C*-glycosyl analogue of lactose is bound by *E. coli* β-galactosidase in an unusual high-energy conformation.[6] In a parallel way, also within the carbohydrate–protein recognition research area, we have been studying the interactions between chitooligosaccharides and hevein domains. Hevein is a small, single chain protein of 43 amino acids, integrated in several related chitin-binding proteins, and chitinases, for example, homo dimeric wheat germ agglutinin (WGA) with each chain constituted by four hevein-like domains.[7] Previous reports from our group[8] demonstrated that hevein domains bind *N*,*N*′-diacetylchitobiose and *N*,*N*′,*N*″-triacetylchitotriose with affinity constants in the millimolar range, and that the binding process is enthalpically driven.[9] We have also described the interaction between hevein domains and *N*-acetylglucosamine-containing oligosaccharides in structural terms with the NMR-derived three-dimensional structure of the protein.[10] The results showed that the oligosaccharide does not modify its typical *syn*-Φ,Ψ global minimum conformation upon binding to the lectin. Following our studies on the interaction of hevein-like domains with chitin-derived oligosaccharides,[7–10] we herein report on the determination of the WGA-bound conformation and *N*,*N*′-diacetyl-4-thiochitobiose by using NMR spectroscopy. The comparison with the bound structure of the *O*-glycoside analogue (**2**) and with the corresponding conformation when free in water solution is also performed. This study represents the first step towards the study of the interaction of non-hydrolyzable chitobiose analogues with chitin-binding lectins.

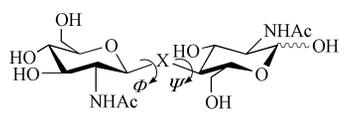

1 X=S
2 X=O

From the glycomimetics' point of view, it is obvious that the substitution of the *exo*- or *endo*-cyclic oxygens by other atoms will result in a change in both the size and the electronic properties of the glycosidic linkage, particularly in the anomeric effects.[11] Thus, it is important to verify whether or not the bound conformation of natural saccharides is maintained by the synthetic analogues. The study of several thioglycosides[12] has shown that due to the different contribution of stereoelectronic and steric effects, pseudoglycosidic bonds may be expected to be conformationally different to *O*-glycosidic linkages. In fact, the C–S bond length (1.78 Å) and C–S–C bond angle (99°) strongly differ from C–O (1.41 Å) and C–O–C (116°).

Results and discussion

Molecular mechanics and dynamics calculations

The adiabatic surfaces calculated for **1** using different force fields (AMBER*, MM2*) are shown in Fig. 1.[13] From these energy surfaces, probability distributions were obtained according to a Boltzmann function. Glycosidic torsion angles are defined as Φ H1′–C1′–X–C4 and Ψ C1′–X–C4–H4. Three different conformational families are found (Table 1). Different distributions are provided by the two force fields. In fact, depending on the force field used, the global minimum is either the *syn*-Φ/*anti*-Ψ or the *syn*-Φ/*syn*-Ψ conformer. In any case, the population values are in contrast with those predicted and experimentally proven for *O*-chitobiose (**2**),[14] for which there is a much higher contribution (>90%) of this *syn*-Φ/*syn*-Ψ conformation. A third conformational family (Fig. 2, *anti*-Φ/*syn*-Ψ, $\Phi = 171 \pm 3$, $\Psi = 2 \pm 4$) is also predicted to exist with *ca.* 5% population. This conformation is below experimental detection for glycoside derivatives, although it has been detected

DOI: 10.1039/b006965p

Table 1 Torsional angle values (Φ,Ψ) of the predicted low energy minima (A, B, C) from MM2* and AMBER*, for compound **1**. The regions around Φ extend *ca*. 20° and around Ψ *ca*. 30°. For the *O*-glycosyl natural compound **2**, the range of populations predicted by AMBER* and MM2* is also given

Conformer	Torsion angle (Φ,Ψ)	Population (%) AMBER-MM2*	Conformer[a]	Torsion angle (Φ,Ψ)	Population (%) MM2*
1-A	51.6/13.4	27–47	**2**-A	50.5/−1.5	92–94
1-B	58.4/−167.8	68–43	**2**-B	21.7/174.2	8–6
1-C	173/1.2	5–10	**2**-C	169.8/4	<1

[a] Conformers A–C: A stands for *syn*-Φ/*syn*-Ψ; B *syn*-Φ/*anti*-Ψ; C *anti*-Φ/*syn*-Ψ.

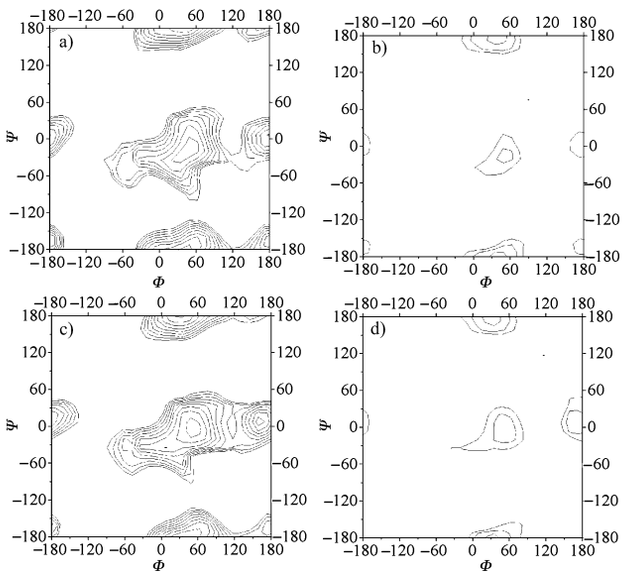

Fig. 1 Steric energy maps (a, c) calculated by the AMBER* and MM2* programs, respectively for **1**. Energy contours are given every 0.5 kcal mol^{-1}. The corresponding population distribution maps (b, d) are also given with contours at 0.65, 2.55, and 10% of population.

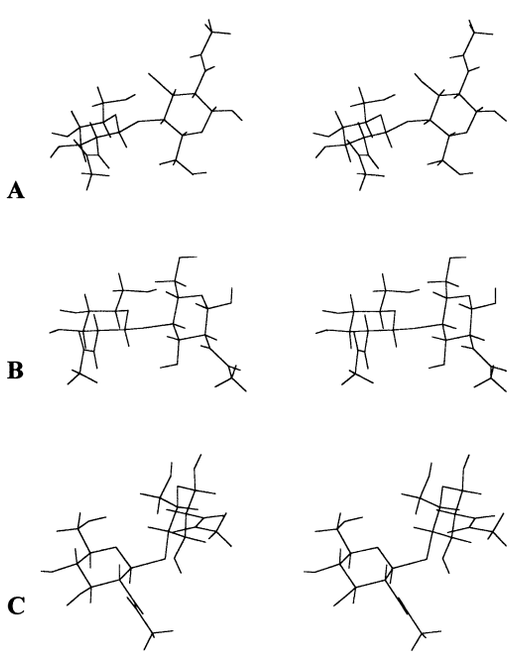

Fig. 2 Simplified stereo views of the major low-energy conformations (from top to bottom, *syn*-Φ/*syn*-Ψ, *syn*-Φ/*anti*-Ψ and *anti*-Φ/*syn*-Ψ) obtained by MM2* calculations for compound **1**. Φ is H1′–C1′–S–C4 and Ψ is C1′–S–C4–H4. For Φ, *syn* conformation is defined as 60°, and the *anti* as 180°.

for the *C*-glycosyl analogue of lactose in solution (*ca*. 5%),[15] and in fact, it has been found in the molecular complex between *C*-lactose and *E. coli* β-galactosidase. Additional information on the conformational stability of the different minima was obtained from MD simulations with the MM3* force field using the continuum GB/SA (Generalized Born solvent-accessible surface area) solvent model for water.[16] Independently from the starting minimum, the calculated trajectories showed several interconversions among the two major energy regions, with minor excursions to the *anti*-Φ region, therefore presenting a clear resemblance to the adiabatic surface described above.

Table 2 ^{1}H-NMR chemical shifts (δ, ppm) of both anomers of **1**

	α-Anomer	β-Anomer
H1	5.25	4.70
H2	3.90	3.66
H3	3.80	3.59
H4	2.92	2.90
H5	4.05	3.65
H6a	3.95	3.80
H6b	4.05	4.06
H1′	4.72	4.72
H2′	3.75	3.75
H3′	3.59	3.59
H4′	3.48	3.48
H5′	3.90	3.90
H6a′	3.75	3.75
H6b′	3.90	3.90

NMR studies

The validity of the theoretical results has been tested using NMR measurements, especially NOEs. The assignment of the resonances was made through a combination of COSY, HSQC, and TOCSY experiments at 500 MHz, recorded under a variety of temperatures to try to avoid signal overlapping. The results are shown in Table 2. The key conformational information was obtained from NOE experiments.[17] 2D-NOESY (see one example in Fig. 3), 2D-ROESY and 1D-DPFGSE NOESY[18] spectra were acquired. Our analysis was performed on the basis of the exclusive[19] interresidue NOEs that unequivocally characterize the *syn*-Φ/*syn*-Ψ, *syn*-Φ/*anti*-Ψ, and *anti*-Φ/*syn*-Ψ regions of the conformational map. For β(1⟶4) saccharides such as **1**, these are H1′–H4 and H1′–H6$_{pro\text{-}S,R}$ (*syn*-Φ/*syn*-Ψ), H1′–H3 (*syn*-Φ/*anti*-Ψ), and H4–H2′ (*anti*-Φ/*syn*-Ψ), respectively. The relevant interresidual proton–proton distances are shown in Table 3 along with the intensity of the experimental NOEs. The data in Table 3 indicate that, for **1**, it is not possible to justify simultaneously all the observed NOEs with just one conformer. At least qualitatively, the presence of NOEs between H1′ and H3 indicate that the minimum *syn*-Φ/*anti*-Ψ is heavily populated in solution. The NOE between H1′ and H4 also indicates the presence of conformer *syn*-Φ/*syn*-Ψ. This is confirmed by the NOEs between H1′ and both H6$_{pro\text{-}R,S}$ protons, since these contacts are exclusive for this minimum. Finally, the existence of conformer *anti*-Φ/*syn*-Ψ can not be confirmed by the NMR data, since the H2′–H4 NOE cannot be detected. From a quantitative point of view, the distances obtained from the molecular mechanics distributions were compared with those

Table 3 Relevant interresidue and ensemble average $\langle r^{-6}\rangle^{-1/6}$ proton–proton distances/Å for **1**. Strong, medium, and weak experimental NOEs are denoted by s, m, and w, respectively. Short distances which would produce observable NOEs are in bold. The estimated error is 15%

Proton pair	Expected distances for conformer (Å)			Ensemble average expected/ NOEs (%)	Experimental NOE intensities
	A	B	C		
H1′–H2′	**3.1**	**3.1**	**3.1**	2.2	w
H1′–H3′	**2.7**	**2.7**	**2.7**	5.5	ms
H1′–H5′	**2.3**	**2.3**	**2.3**	11.4	s
H1′–H4	**2.4**	4.1	3.3	1.6	mw
H1′–H5	5.0	**2.3**	4.3	2.0	w
H1′–H3	4.6	**2.1**	4.5	2.2	w
H1–H5	**2.4**	**2.4**	**2.4**	9.4	s
H1–H3	**2.7**	**2.7**	**2.7**	5.2	ms

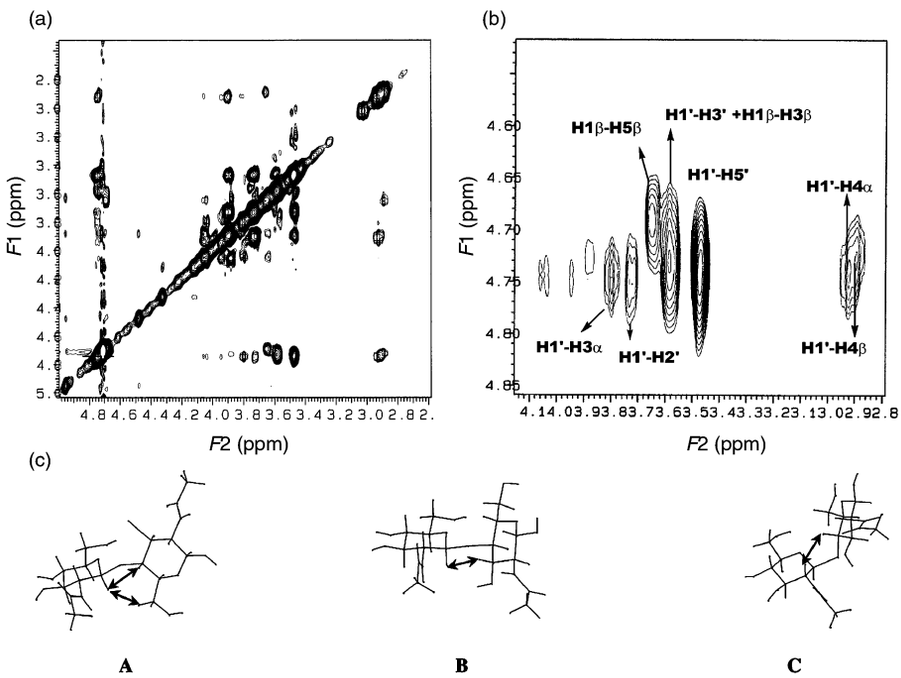

Fig. 3 a) 2D-NOESY spectrum of **1** at pH 7.0, 500 MHz, 303 K, D_2O, with a mixing time of 600 ms. b) Key NOEs in the expanded anomeric region are noted. c) Schematic view of the short interproton distances for the low energy minima of **1** that correspond to the observed NOEs. A) *syn*-Φ,Ψ (H1′–H4, H1′–H6ab), B) *syn*-Φ, *anti*-Ψ (H1′–H3), and C) *anti*-Φ, *syn*-Ψ (H2′–H4).

estimated experimentally, by using a full relaxation matrix approach.[17] It can be observed that the agreement is satisfactory, and that the population of **1** can be explained with a 65 : 30 : 5 conformational distribution among the three mentioned minima, *syn*-Φ/*anti*-Ψ, *syn*-Φ/*syn*-Ψ, and *anti*-Φ/*syn*-Ψ, respectively, much closer to the AMBER* distribution than to the MM2*-based one. Nevertheless, it has to be stated, according to Neuhaus and Williamson,[17] that *the ability to fit NOE data using predicted conformations cannot be taken to mean that those conformations are necessarily those that are present; other choices might also fit the NOE data*.

In conclusion, all the molecular mechanics and NMR results have allowed us to demonstrate the different conformational behaviour of *S*-chitobiose with respect to its *O*-analogue. Summarising, the minima of **1** adopt *exo*-anomeric conformations around Φ, but the orientations around the aglyconic bond Ψ are rather different between *S*- and *O*-glycosyl compounds. The major conformer for *O*-glycoside is centered at the *syn*-Ψ region. However, for **1** the *anti* conformer has a larger population. The participation of conformers *anti*-Φ, for **1**, with a torsional variation of 120° upon Φ angle, very unusual for β-*O*-glycosides, can not be detected experimentally, although it is predicted by the calculations. Therefore, *S*-glycosides may also display significant conformational variations around the Ψ angle as also observed for β-*C*-lactosides. Similar results have

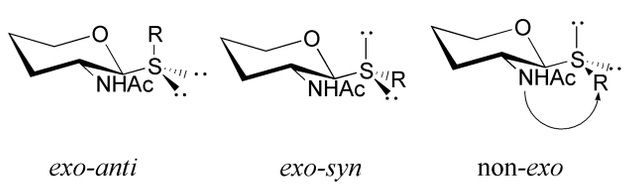

Fig. 4 Schematic representation of the three basic orientations around ϕ angle in *N*-acetylglucopyranosides. The 1,3-*syn* diaxial type interactions between the NHAc group and the aglycone are indicated.

also been observed for other *S*-glycosides with different stereochemistries at their glycosidic linkages. The variations in bond lengths and angles may provide the answer to the much higher flexibility of **1** *versus* its natural *O*-analogue. For **1**, with no acetal-type moiety, the *exo*-anomeric type stereoelectronic stabilization is no longer possible. Therefore, the explanation for the *exo*-anomeric preference around Φ should mainly reside in steric effects, probably 1,3-type interactions. In fact, for the regular $^4C_1$(D) chairs, there is a 1,3-type interaction between one equatorially substituted C2 (GlcNAc-series, as **1**) and the aglycone, when the non-*exo*-anomeric (non-*exo*) conformation is considered (Fig. 4). There are no such steric interactions for the *exo*-anomeric (*exo*) and the *anti* conformations. Therefore, this interaction is probably the origin for the strong preference of the *exo*-anomeric orientation in **1**.[20] For *O*-glycosides, such

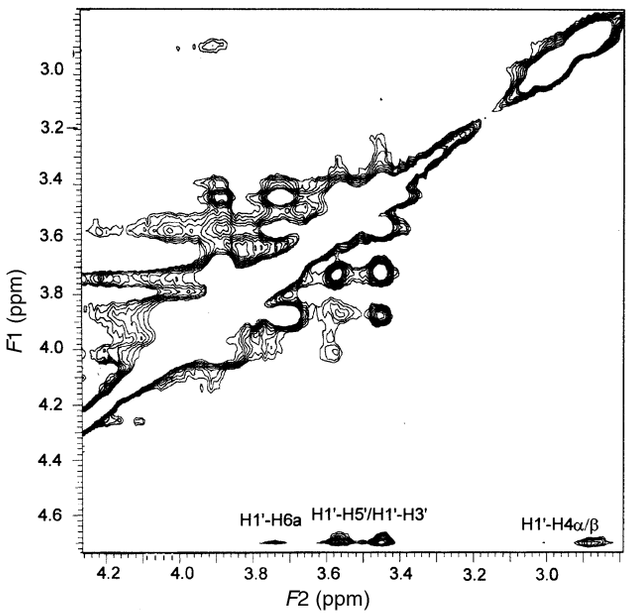

Fig. 5 Expansion of the key regions of the 500 MHz ^{1}H-NMR NOESY spectrum recorded for **1** bound to WGA for a molar ratio of 24 : 1. Relevant cross peaks are indicated. The *anti*-Ψ (H1′–H3) and *anti*-Φ (H2′–H4) cross peaks have basically disappeared. The strong H1′–H4 NOE indicate the presence of the *syn*-Φ,Ψ as the major conformer.

as **2**, it is obvious that the stereoelectronic effect will be additionally superimposed, with a subsequent further stabilization of the *exo*-anomeric orientation, thus providing the explanation for the basically unique conformation around the Φ angle of the natural oligosaccharides.[20,21]

The bound conformation to WGA

TR-NOE experiments were performed to deduce the bound conformation of **1** to WGA, with four hevein like domains. For ligands which are not bound tightly and exchange with the free ligand at a reasonably fast rate, the transferred nuclear Overhauser enhancement (TR-NOE) experiment provides an adequate means to determine the conformation of the bound ligand.[22,23] This approach has been recently applied to several studies of lectin- and antibody-bound oligosaccharides.[24] Notably, the conditions required to monitor TR-NOEs appear to be satisfied frequently by sugar receptors. The reason for this favorable situation is a result of a combination of factors. Notably, these interactions are not extremely strong, there is fast exchange between the free and the bound states of the ligand, and the perturbations of the conformational equilibrium of a given oligosaccharide upon binding to a protein are accessible to observation by TR-NOE. TR-NOESY experiments (Fig. 5) were performed at different mixing times giving rise to strong and negative NOEs, as expected for ligand binding. The comparison between the NOESY spectra recorded in the absence and in the presence of the lectin showed important and clear differences. Some of the cross peaks in the NOESY spectrum of the free ligand did not show up in the TR-NOESY spectrum of the complex. In particular, both H1′–H3 and H2′–H4 NOEs disappear, evidence that neither the *syn*-Φ/*anti*-Ψ conformation (global minimum) nor the *anti*-Φ/*syn*-Ψ conformation is recognized by the lectin. By contrast, the H1′–H4 NOE which is displayed at medium intensity for the free ligand is now the strongest interresidual NOE in the spectrum. These features clearly indicate that the bound conformation belongs to the local minimum of **1**, *syn*-Φ/*syn*-Ψ family. This cross peak showed a different sign to the diagonal peaks in TR-ROESY experiments, thus excluding the possibility of protein-relayed or spin diffusion mediated correlations.

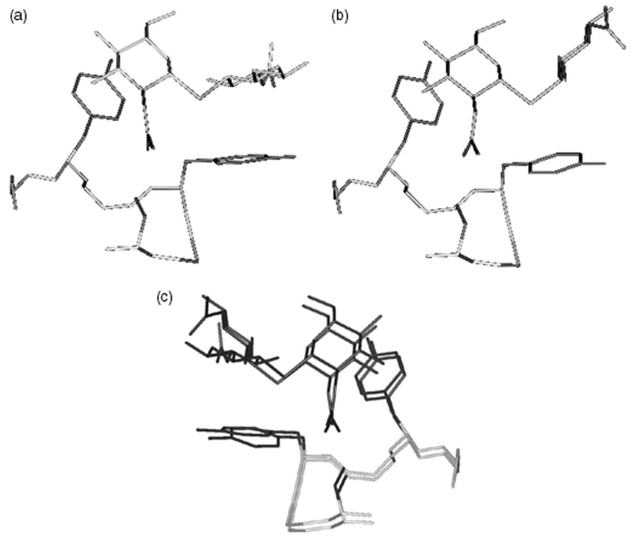

Fig. 6 View of the calculated three dimensional structures of WGA complexed with the two more stable conformers of **1** after docking studies. A) left, with the *anti*-Ψ conformer. B) right, with the *syn*-Ψ conformer. C) bottom, a superimposition of both. The relevant intermolecular hydrogen bonds and stacking interactions are observable.

Therefore, these NMR-based experimental results indicate that WGA recognises a local minimum of *S*-chitobiose, which corresponds to the global minimum of the *O*-glycoside, **2**. Therefore, this lectin selects the same conformation of the *O*- and *S*-glycosyl compounds. The bound conformation has a medium size population for free **1** (35%, see above), while it is the major one (>90%) for natural chitobiose **2** in aqueous solution. Taking into account the energetic differences between the local energy and the global minimum conformer of the *S*-analogue in solution, which amounts to about 4 kJ mol^{-1}, it seems that the lectin shows an intrinsic binding energy of at least this magnitude. The three dimensional architecture of the binding site of hevein domains can easily explain why the *syn*-Φ,Ψ conformer is the bound one. In the three dimensional structure of the known hevein–*N*,*N*′-diacetylchitobiose complexes,[7–10] the non-reducing GlcNAc residue occupies subsite +1, and the non-reducing acetamido methyl group shows non-polar contacts with two aromatic residues Tyr30 and Tyr21, and, in addition, there are important hydrogen bonds which confer stability on the complex: one between the non-reducing sugar acetamido group and Ser19 and a second one involving C3–OH and Tyr30. One additional interaction is observed between the α-face of the reducing GlcNAc moiety at subsite +2, and the plane of the aromatic ring of Tyr or Trp21. For the *S*-glycosyl analogue **1**, these interactions can only take place if thiochitobiose adopts the *syn*-Φ,Ψ conformation (Fig. 6), otherwise, one or several of the above mentioned interactions would not take place. Therefore, the lectin selects one of the existing conformations in solutions of the glycomimetic.

Conclusions

The results presented herein clearly show that the flexibility around the glycosidic linkages of pseudoglycosides may be determined by NMR experiments in combination with molecular mechanics calculations. In addition, the conformational changes observed, especially for *S*-glycosides, also reflect the small energy barriers between the different energy regions. Thus, conformations different from the major one existing in solution may be bound by the binding site of proteins without major energy conflicts, as shown herein. These results, along with those previously obtained by us for *C*-glycosides are important for drug design. For the binding of a flexible compound to a protein, usually one of the existing conformations

should be selected out of the ensemble.[25] Therefore, a negative binding entropy will be expected, thus decreasing the energy of binding.[26] Consequently, the flexibility of *S*-disaccharides may be a limitation in their use as therapeutic agents. Nevertheless, these compounds may be excellent probes to study the combining sites of proteins and enzymes. They may also serve as test compounds to compare conformational properties of oligosaccharides.

Experimental

Materials

WGA was obtained from commercial sources (Sigma, Aldrich).

Compounds

The synthesis of *N*,*N*′-diacetylthiochitobiose will be described elsewhere.

Molecular mechanics and dynamics calculations

Molecular mechanics and dynamics calculations were performed using the MM2*, MM3*, and AMBER* force fields as implemented in MACROMODEL 4.5.[27] Φ is defined as H1′–C1′–X–C4 and Ψ as C1′–X–C4–H4. Thus, the atoms of the non-reducing end are primed. Only the *gg* and *gt* orientations of the lateral chain were used for the GlcNAc moieties.[28] Separate calculations for a relative permittivity $\varepsilon = 80$ D and for the continuum GB/SA solvent model were performed. Two different sets of calculations were considered with either *anti*- or *syn*-type orientations for the H2–C2–NH torsion angles of the acetamide moiety. For both sets, the potential energy maps were calculated first for the disaccharides: relaxed (Φ,Ψ) potential energy maps were calculated as described. Four initial geometries were considered, cc, cr, rr and rc, obtained by combining the positions r (reverse clockwise) and c (clockwise) for the orientation of the secondary hydroxy groups of both pyranoid moieties. The first character corresponds to the non-reducing moiety, and the second one, to the reducing moiety. In total, 16 maps were calculated. The previous step involved the generation of the corresponding rigid residue maps by using a grid step of 18°. Then, every Φ,Ψ point of this map was optimised using 200 steepest descent steps, followed by 1000 conjugate gradient iterations. From these relaxed maps, adiabatic surfaces were built, and the probability distributions calculated for each ϕ,Ψ point according to a Boltzmann function at 303 K.

The conformational stability of the energy minima was explored through molecular dynamics (MD) simulations.[29] The three most relevant energy minima were used as starting geometries for MD at 300 K, with the GB/SA solvent model, and a time step of 1 fs. The equilibration period was 100 ps. After this period, structures were saved every 0.5 ps. The simulation time was 1 ns for every run. Average distances between intra- and inter-residue proton pairs were calculated from the dynamics simulations.

NMR spectroscopy

NMR experiments were recorded on a Varian Unity 500 spectrometer, using an approximately 2 mg mL^{-1} solution of the pseudodisaccharides at different temperatures. Chemical shifts are reported in ppm, using external TMS (0 ppm) as references. The double quantum filtered COSY spectrum was performed with a data matrix of 256 × 1K to digitize a spectral width of 2000 Hz. Sixteen scans were used with a relaxation delay of 1 s. The 2D TOCSY experiment was performed using a data matrix of 256 × 2K to digitize a spectral width of 2000 Hz; 4 scans were used per increment with a relaxation delay of 2 s. MLEV 17 was used for the 100 ms isotropic mixing time. The one-bond proton–carbon correlation experiment was collected in the ^{1}H-detection mode using the HSQC sequence and a reverse probe. A data matrix of 256 × 2K was used to digitize a spectral width of 2000 Hz in F_2 and 10000 Hz in F_1. Four scans were used per increment with a relaxation delay of 1 s and a delay corresponding to a *J* value of 145 Hz. A BIRD pulse was used to minimize the proton signals bonded to ^{12}C. ^{13}C decoupling was achieved by the WALTZ scheme.

NOESY experiments were performed with the selective 1D double pulse field gradient spin echo (DPFGSE) module, using four different mixing times, namely 150, 300, 450, and 600 ms. 2D NOESY, 2D-ROESY, and 2D-T-ROESY experiments were also performed with the same mixing times, and using 256 × 2K matrixes.

NOE calculations

NOESY spectra were simulated according to a complete relaxation matrix approach, following the protocol previously described,[30] using four different mixing times (between 150 and 600 ms). The spectra were simulated from the average distances $\langle r^{-6} \rangle_{kl}$ calculated from the relaxed energy maps at 303 K with both force fields. Given the variation of the distribution provided by both force fields (see Tables), following this protocol it is possible to deduce an actual population distribution by comparison with the experimental data. Isotropic motion and an external relaxation of 0.1 s^{-1} were assumed. A τ_c of 95 ps was used to obtain the best match between experimental and calculated NOEs for the intraresidue proton pairs (H1′–H3′, H1′–H5′, and/or H1–H3). All the NOE calculations were automatically performed by a home made program, available from the authors upon request.

TR-NOE experiments

The ligand was exposed to repeated cycles of freeze drying with D_2O, and transferred to the NMR tube to give a final concentration of 0.5 mM. TR-NOESY experiments were performed with mixing times of 200 ms and 300 ms, for 11 : 1 and 22 : 1 molar ratios of ligand : lectin. In all cases, line broadening of the sugar protons was monitored after the addition of the ligand. TR-ROESY experiments were also carried out to detect spin diffusion effects (not shown). A continuous wave spin lock pulse was used during the 250 ms mixing time. Key NOEs were shown to be direct cross peaks, since they showed a different sign to the diagonal peaks.

Molecular modeling

Protein coordinates were taken from the NMR structure of the B-domain of WGA, recently described by us.[10] Glycosidic torsion angles of the glycomimetic were set to those described above for the *syn* and *anti* minima. Atomic charges were AMBER charges. The starting orientation of the non-reducing residue was chosen to match that of the NMR structure of the WGA-B–chitotriose complex. Only one protein domain was considered (B-domain) for the calculations. For the complex, all energy calculations were carried out using the AMBER 5.0 force field. A relative permittivity of 4*r was employed. A template force potential was introduced to avoid major movements of the polypeptide backbone during the calculations. The pseudodisaccharide and the amino acid lateral chains were left free during the minimization processes. No cutoffs for non-bonding interactions were used. The three major conformers: *syn*-Φ, *anti*-Ψ, and *anti*-Φ were generated with two initial Φ and Ψ values. Energy minimizations were then conducted on the six complexes using 2000 conjugate gradient iterations. The *anti*-Φ conformer generated important steric conflicts with the polypeptide chain and gave rise to a final *syn*-Φ conformation.

Acknowledgements

This paper is dedicated to the late Professor Göran Magnusson for his relevant contributions to carbohydrate chemistry and to

the study of sugar–protein interactions. Financial support by DGICYT (Grant PB96-0833) is gratefully acknowledged. J. L. A. thanks CAM and MEC for fellowships. A. G. thanks Gobierno Vasco for a fellowship, and F.-I. A. thanks Professor J. Gelas for his support.

References

1 (*a*) *Glycosciences: Status and Perspectives*, eds. H.-J. Gabius and S. Gabius, Chapman & Hall, London, 1997; (*b*) *Chemistry of C-glycosides*, eds. W. Levy and C. Chang, Elsevier, Cambridge, 1995; (*c*) H. Driguez, *Top. Curr. Chem.*, 1997, **187**, 85; (*d*) J. S. Andrews and B. M. Pinto, *Carbohydr. Res.*, 1995, **270**, 51; (*e*) H. Yuasa and H. Hashimoto, *Rev. Heteroat. Chem.*, 1999, **19**, 35.

2 (*a*) B. A. Johns, Y. T. Pan, A. D. Elbein and C. R. Johnson, *J. Am. Chem. Soc.*, 1997, **119**, 4856; (*b*) for a special volume on glycosciences see H.-J. Gabius and F. Sinowatz, *Acta Anat.*, 1998, **161**, 1.

3 S. Ogawa, K. Hirai, T. Odagiri, N. Matsunaga, T. Yamazaki and A. Nakajima, *Eur. J. Org. Chem.*, 1998, **1**, 1099; and references therein.

4 M. S. Searle and D. H. Williams, *J. Am. Chem. Soc.*, 1992, **114**, 10690.

5 E. Montero, M. Vallmitjana, J. A. Perez-Pons, E. Querol, F. J. Jiménez-Barbero and F. J. Cañada, *FEBS Lett.*, 1998, **421**, 243.

6 J. F. Espinosa, E. Montero, A. Vian, J. L. Garcia, H. Dietrich, M. Martín-Lomas, R. R. Schmidt, A. Imberty, F. J. Cañada and J. Jiménez-Barbero, *J. Am. Chem. Soc.*, 1998, **120**, 1309.

7 (*a*) C. S. Wright, *J. Mol. Biol.*, 1984, **178**, 91; (*b*) X. Gidrol, H. Chrestin, H.-L. Tan and A. Kush, *J. Biol. Chem.*, 1994, **209**, 9278.

8 J. L. Asensio, F. J. Cañada, M. Bruix, A. Rodriguez-Romero and J. Jiménez-Barbero, *Eur. J. Biochem.*, 1995, **230**, 621.

9 J. L. Asensio, H.-C. Siebert, F. J. Cañada, C.-W. von der Lieth, J. Laynez, M. Bruix, J J. Beintema, H.-J. Gabius and J. Jiménez-Barbero, *Proteins Struct. Funct. Genet.*, 2000, **40**, 218.

10 J. L. Asensio, F. J. Cañada, H.-C. Siebert, J. Laynez, A. Poveda, P. M. Nieto, U. M. Soedjanaamadja, H.-J. Gabius and J. Jiménez-Barbero, *Chem. Biol.*, 2000, **7**, 529.

11 (*a*) R. U. Lemieux, S. Koto and D. Voisin, *ACS Symp. Ser.*, 1979, **87**, 17; (*b*) G. R. J. Thatcher, *The Anomeric Effect and Associated Stereoelectronic Effects*, American Chemical Society, Washington, DC, 1993; (*c*) I. Tvaroska and T. Bleha, *Adv. Carbohydr. Chem. Biochem.*, 1989, **47**, 45; (*d*) A. J. Kirby, *The Anomeric Effect and Related Stereoelectronic Effects at Oxygen*, Springer-Verlag, Heidelberg, Germany, 1983.

12 (*a*) K. Bock, J. O. Duus and S. Refn, *Carbohydr. Res.*, 1994, **253**, 51; (*b*) A. Geyer, G. Hummel, T. Eisele, S. Reinhardt and R. R. Schmidt, *Chem. Eur. J.*, 1996, **2**, 981; (*c*) U. Nilsson, R. Johansson and G. Magnusson, *Chem. Eur. J.*, 1996, **2**, 295; (*d*) B. Aguilera, J. Jiménez-Barbero and A. Fernández-Mayoralas, *Carbohydr. Res.*, 1998, **308**, 19; (*e*) E. Raimbaud, A. Buleon and S. Perez, *Carbohydr. Res.*, 1992, **227**, 351; (*f*) E. Montero, A. García-Herrero, J. L. Asensio, H. Hirai, S. Ogawa, F. J. Cañada and J. Jiménez-Barbero, *Eur. J. Org. Chem.*, 2000, 1945.

13 (*a*) A general survey of conformation of carbohydrates and analogues is presented in: *Computer Modelling of Carbohydrate Molecules*, eds. A. D. French and J. W. Brady, American Chemical Society, Washington, DC, 1990; for a detailed description of conformational analysis of carbohydrates using NMR and calculations, see (*b*) T. Peters and B. M. Pinto, *Curr. Opin. Struct. Biol.*, 1996, **6**, 710; (*c*) A. Imberty, *Curr. Opin. Struct. Biol.*, 1997, **7**, 617.

14 J. F. Espinosa, J. L. Asensio, M. Bruix and J. Jiménez-Barbero, *An. Quim.*, 1996, **92**, 320.

15 (*a*) J. F. Espinosa, M. Martín-Pastor, J. L. Asensio, H. Dietrich, M. Martín-Lomas, R. R. Schmidt and J. Jiménez-Barbero, *Tetrahedron Lett.*, 1995, **36**, 6329; (*b*) J. F. Espinosa, F. J. Cañada, J. L. Asensio, M. Martín-Pastor, H. Dietrich, M. Martín-Lomas, R. R. Schmidt and J. Jiménez-Barbero, *J. Am. Chem. Soc.*, 1996, **118**, 10862.

16 W. C. Still, A. Tempczyk, R. C. Hawley and T. Hendrickson, *J. Am. Chem. Soc.*, 1990, **112**, 6127.

17 D. Neuhaus and M. P. Williamson, *The Nuclear Overhauser Effect in Structural and Conformational Analysis*, VCH Publishers, New York, 1989.

18 K. Stott, J. Stonehouse, J. Keeler, T.-L. Hwang and A. J. Shaka, *J. Am. Chem. Soc.*, 1995, **117**, 4199.

19 J. Dabrowski, T. Kozar, H. Grosskurth and N. E. Nifant'ev, *J. Am. Chem. Soc.*, 1995, **117**, 5534.

20 J. L. Asensio, F. J. Cañada, A. García, M. T. Murillo, A. Fernández-Mayoralas, B. A. Johns, J. Kozak, Z. Zhu, C. R. Johnson and J. Jiménez-Barbero, *J. Am. Chem. Soc.*, 1999, **121**, 11318.

21 J. L. Asensio, F. J. Cañada, X. Cheng, N. Khan, D. R. Mootoo and J. Jiménez-Barbero, *Chem. Eur. J.*, 2000, **6**, 1035.

22 (*a*) F. Ni, *Prog. Nucl. Magn. Reson. Spectrosc.*, 1994, **26**, 517; (*b*) V. L. Bevilacqua, D. S. Thomson and J. H. Prestegard, *Biochemistry*, 1990, **29**, 5529; (*c*) V. L. Bevilacqua, Y. Kim and J. H. Prestegard, *Biochemistry*, 1992, **31**, 9339.

23 A. Poveda and J. Jiménez-Barbero, *Chem. Soc. Rev.*, 1998, **27**, 133.

24 J. Jiménez-Barbero, J. L. Asensio, F. J. Cañada and A. Poveda, *Curr. Opin. Struct. Biol.*, 1999, **9**, 549.

25 For conformational selection in carbohydrate recognition by proteins, in addition to ref. 11, see (*a*) M. Gilleron, H.-C. Siebert, H. Kaltner, C. W. von der Lieth, T. Kozar, K. M. Halkes, E. Y. Korchagina, N. V. Bovin, H.-J. Gabius and J. F. G. Vliegenthart, *Eur. J. Biochem.*, 1998, **249**, 27; (*b*) J. L. Asensio, J. F. Espinosa, H. Dietrich, F. J. Cañada, R. R. Schmidt, M. Martín-Lomas, S. André, H.-J. Gabius and J. Jiménez-Barbero, *J. Am. Chem. Soc.*, 1999, **121**, 8995.

26 For different implications of conformational restriction of the ligand upon protein binding, see (*a*) D. R. Bundle, R. Alibés, S. Nilar, A. Otter, M. Warwas and P. Zhang, *J. Am. Chem. Soc.*, 1998, **120**, 5317; (*b*) N. Navarre, N. Amiot, A. H. van Oijen, A. Imberty, A. Poveda, J. Jiménez-Barbero, A. Cooper, M. A. Nutley and G. J. Boons, *Chem. Eur. J.*, 1999, **5**, 2281.

27 F. Mohamadi, N. G. J. Richards, W. C. Guida, R. Liskamp, C. Caufield, G. Chang, T. Hendrickson and W. C. Still, *J. Comput. Chem.*, 1990, **11**, 440; the MM3* force field (N. L. Allinger, Y. H. Yuh and J. H. Lii, *J. Am. Chem. Soc.*, 1989, **111**, 8551) implemented in MACROMODEL differs of the regular MM3 force field in the treatment of the electrostatic term since it uses charge–charge instead of dipole–dipole interactions. The AMBER* force field used in this work is parametrised for sugars: S. W. Homans, *Biochemistry*, 1990, **29**, 9110.

28 K. Bock and J. Duus, *J. Carbohydr. Chem.*, 1994, **13**, 513.

29 For a detailed description of conformational analysis of carbohydrates using MD simulations, see R. J. Woods, *Curr. Opin. Struct. Biol.*, 1995, **5**, 591.

30 J. L. Asensio and J. Jiménez-Barbero, *Biopolymers*, 1995, **35**, 55.